E. Paese[1]
epaese@terra.com.br
M.Geier[2]
R. P. Homrich[1]
J. L. Pacheco[2]

Universidade Federal do Rio Grande do Sul
[1]Programa de Pós-Graduação em Eng. Elétrica
Av. Osvaldo Aranha, 103
90035-190 Porto Alegre, RS, Brazil
[2]Programa de Pós-Graduação em Eng. Mecânica
Rua Sarmento Leite, 425 – 2º Andar
90.050-170 Porto Alegre, RS, Brazil

Simplified Mathematical Modeling for an Electromagnetic Forming System with Flat Spiral Coil as Actuator

This study presents mathematical modeling and calculation procedure for problems of electromagnetic forming of thin circular metal sheets using a flat spiral coil as actuator. The method based on the Biot-Savart Law focuses specifically on the calculation of the electromagnetic field generated by the flat coil and analysis of the circuit that models the electromagnetic forming system to the initial time, before the plastic deformation of the sheet. The solution of magnetic induction integral equations is performed by numerical methods specifically with the use of Matlab® software, providing important information that serves as feedback for system design. Free bulging experiments were performed to demonstrate a good relationship with the mathematical model predictions for electrical discharge current in the coil and induced currents in the metal sheet, behavior of the transient electromagnetic force between coil and workpiece, and distribution of magnetic field, electromagnetic density force along the coil.
Keywords: *mathematical model, high speed forming, electromagnetic forming*

Introduction

Sheet metal forming is an important manufacturing process because of its high production rate and low cost. It is a fundamental technology in automotive, heavy vehicle and aerospace industries. Current initiatives in automotive industry are driving a need for stronger and lighter automotive panels together with complex shapes. Light metals, such as high strength steel, aluminum alloys, magnesium, are developed to reduce overall body weight and improve the fuel consumption. Their lower formability has pushed the current sheet metal stamping technologies to their limits (Shang, 2006).

Sheet metal forming process converts an initially flat metal sheet into a useful part with the desired shape. The formability of a sheet metal is a complex measure of its ability to accommodate the strains for the desired shape without failure in a forming process. Formability depends not only on the properties of the sheet metal, but also on the process factors in a practical forming operation (Shang, 2006).

Several manufacturing methods were developed to improve the formability of stamping, such as better material properties of sheet metals, varied blank holder force, multi-point die-cushion technology to apply the blank holder pressure at multiple points with different intensities, active control of material flow at the entrance die (active drawbead), lubrication and optimization of initial blank design. These can be applied together or individually (Shang, 2006).

Nowadays the sheet metal forming process is traditionally done in complex machines, specially designed, expensive, high mechanical complexity and sophisticated control fluid mechanical systems. Moreover, they use complex stamping tools with punches and dies, extractors, set of blank holders that may or may not include drawbeads, springs, columns, guides, etc. The production rates are in constant study to improve productivity and product quality. The finish of stamping process depends on a number of factors such as previous finish of blank and tool, lubricant used, the tooling clearances, etc. The changeover times and adjustments of stamping tools to production are also long and should be reduced.

High velocity forming operations are considered to be operations where the workpiece velocities typically exceed 100 m/s. These methods include techniques such as explosive forming and electromagnetic forming. These techniques are distinct from most other metal forming methods in that the workpiece is accelerated to a high velocity by the chemical, mechanical or electrical force, and the kinetic energy of the workpiece is significant (Kamal, 2005).

High velocity techniques generally are applied where conventional methods of metal forming fail. Looking at the current technological possibilities there are a number of methods for high velocity forming mainly based on the source of energy used for obtaining high velocities. The common ones are (Kamal, 2005):

- Pneumatic-mechanical: It uses the energy stored in a compressed gas at high pressure, which expands on a punch or liquefied gas, which expands directly over the plate. The latter requires extremely high pressures impractical from the standpoint of practical. The use of punch on the other hand, refers to even finish of traditional stamping process. Was there still a productivity gain, but with doubtful quality and yet it would have complex components.
- Explosive forming: In this process the energy liberated due to the detonation of an explosive is used to form the desired configuration. In general, a metal sheet is placed on a die. The die cavity is vacuumed and the assembly is placed in water. An explosive charge is detonated under water pushing the sheet in the die. The charge used is small, but is capable of exerting tremendous forces on the workpiece and this system is suitable for bigger pieces constructed of high strength materials such as those found in the arms industry and aerospace. The major limitation of this process, however, is law and security in transport, storage and handling of explosives, resulting in a severe limitation to industrial application in large scale.
- Electrohydraulic forming: In principle is very similar to explosive forming except that it uses an electric arc discharge to convert electrical energy to mechanical energy through from gases produced by the hydrolysis of water. The spark can be generated by the same type of bank capacitor used in electromagnetic forming. There are difficulties of pressure control, leakage and noise produced. The work cycles are too long for a good productivity.
- Electromagnetic forming: In this process the deformation is carried out by driving a large pulsed current through a conductive coil in close proximity to a metal workpiece. According to Motoasca (2003), in the conventional processes of stamping the typical speed of deformation is about 0.1 m/s, while in the process at high speed it can reach a few hundred meters per second, including the electromagnetic forming

Paper received 19 August 2010. Paper accepted 28 February 2011.
Technical Editor: Anselmo Diniz

process. This means that the piece is deformed quickly, in order of microseconds. This can generate short work cycles, because the rest of the cycle is charging capacitors, feeding the workpiece in the tools and removal of stamping part. According to Boutana (2008), depending on the configuration coil and the workpiece, this process can be used for compression or expansion of tubular components or forming flat metal sheet in desired shape.

An electromagnetic forming system is essentially a mutual induction system composed of an actuator coil and a conductive workpiece (Takatsu et al., 1988). This process is based on a repulsive force generated by the magnetic fields opposite in adjacent conductors. The transient magnetic field induces eddy currents in the metal sheet, creating an opposite magnetic field. Intense and fast repulsive forces will act on the workpiece, accelerating it at high speed (Mamalis et al., 2006).

Several studies have started from this premise, but most involve specific situations for deformation of tubular parts by solenoid coils, while few studies have analyzed sheet metal forming by planar coils (Takatsu et al., 1988; Meriched, 2000).

The mechanical and electromagnetic phenomena of the process are strongly interrelated, and the deformation of the sheet metal affects the magnetic field and, consequently, the Lorentz's forces developed. An approximate but more realizable approach is to treat the process as a loosely coupled problem, disregarding the influence of deformation of the workpiece in the evolution of the magnetic field, and then apply the forces generated by the electromagnetic field in the mechanical problem (Mamalis et al., 2006).

The electromagnetic forming system has many advantages that make it an attractive alternative to conventional forming systems (hydraulic, mechanic, etc.) or even to other impulsive methods (mechanical, chemical or electrical forming) (Motoasca, 2003; Boutana, 2008). As opposed to most conventional forming systems, during electromagnetic forming, there is no mechanical contact with the workpiece, so lubricants are not needed and the process is cleaner and it is possible stamping parts with previous finish of the blank. The energy transferred is established through the electromagnetic field; the electromagnetic forming process can be carried out in air even vacuum.

The formability limits increase during electromagnetic forming due to high deformation velocity and the principal advantage of electromagnetic forming is its controllability and repeatability, as most of the high velocity process, while the required equipment is relatively simple. Besides many advantages, electromagnetic forming has also some disadvantages: it needs special safety precautions (high voltage of operation) and the required equipment is still expensive. In practice, there are size limitations for workpieces to be formed. During the last few decades, an increasing need to produce high strength components more economically than by conventional forming caused renewed interest in electromagnetic forming (Motoasca, 2003).

This work will show a mathematical model of the electromagnetic forming system and numerical methods for solving a specific problem at the initial time before plastic deformation of circular metal sheets by using a flat spiral coil. The method used approximates the flat spiral coil for circular and coaxial conductors, and the sheet metal is discretized in elementary segments of circular and coaxial conductors. The magnetic field produced can be calculated by applying the law of Biot-Savart. This discretization of the workpiece allows the calculation of the electromagnetic coupling between actuator coil and workpiece. The system to be represented by a set of differential equations where the electromagnetic problem is formulated in terms of the magnetic field and the electrical problem is a circuit with mutual inductances. Experimental results are also presented for different thicknesses of aluminum plates and the results are compared with numerical solution of mathematical model in Matlab software.

The main objective of this paper is to propose a simplified model of an electromagnetic forming system configured with a flat spiral coil as actuator for experimental or industrial application, differing form others already presented (Takatsu et al., 1988; Meriched, 2000). At first, this model is based on the law of Biot Savart, and solves the obtained integrals by numerical methods implemented in an algorithm in software Matlab. This methodology isn't restricted to the analysis of the electromagnetic process, serving also as basis for the design of several components of the electromagnetic forming system presented in this paper (such as capacitor banks, the main discharge switch, buses, etc) and providing information of the discharged current in actuator coil, the induced current in workpiece, and the electromagnetic force and its distribution along the workpiece. Also, another special feature from the proposed model is the possibility to change the process parameters and easily identify its influences as the employed theory in the construction of this algorithm is clearly identified in it.

Nomenclature

A = *area, mm2*
B = *magnetic flux density, T*
C = *capacitance, μF*
D = *diameter, mm*
d = *distance between workpiece and actuator coil, mm*
Fe = *electromagnetic force (Lorentz's force), N*
I = *electric current, A*
L = *self inductance, H*
M = *mutual inductance, H*
n = *number of windings of the actuator coil*
P = *pitch, mm*
R = *electric resistance, Ω*
t = *thickness of workpiece, mm*
U = *energy, J*
V = *electric potential, V*

Greek Symbols

μ_0 = *magnetic permeability of the free space* $= 4\pi 10^{-7}$ *H / m*
α = *angle between component in the direction x and y*
Φ = *magnetic flux, Wb*
λ = *flux linkage, Wb*
ρ = *resistivity,* $\Omega \cdot m$

Subscripts

a = *relative to actuator coil*
c = *relative to capacitor bank*
m = *relative to coaxial circular elementary conductor* m^{th} *of workpiece*
n = *relative to coaxial circular elementary conductor* n^{th} *of workpiece*
o = *relative to outer, external*
r = *relative to radial direction in the system of cylindrical coordinates or component*
α = *relative to angular direction in the system of cylindrical coordinates or component*
w = *relative to workpiece*
x = *relative to direction of the axis x in the system of coordinates or component*
y = *relative to direction of the axis y in the system of coordinates or component*
z = *relative to direction of the axis z in the system of coordinates or component*

Description of the Electromagnetic Problem

A schematic model of the system analyzed is shown in Fig. 1, which shows a circular clamped metal sheet is placed above a flat spiral coil connected to a charged capacitor. The calculations of the electromagnetic problem use a method based on discretization of the metal sheet in a number of circular elementary conductors for axisymmetric configuration.

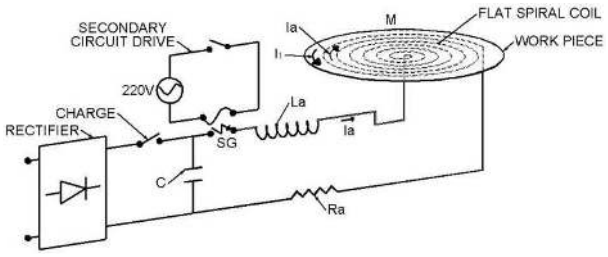

Figure 1. Scheme of the electromagnetic forming system.

The transient electromagnetic problem can be separated in a RLC primary circuit coupled with secondary RL circuit (Kamal, 2005; Shang, 2006). The discharge of the capacitor in the primary circuit can be written in ordinary differential equations:

$$\frac{d}{dt}\left(L_a I_a + M I_1\right) + R_a I_a + V_c = 0 \tag{1}$$

$$I_a = C\frac{dV_c}{dt} \tag{2}$$

where L_a, R_a and V_c are the self-inductance, resistance of actuator coil and electric potential in capacitor bank. M is the mutual inductance between the actuator coil and workpiece. I_a and I_1 are the discharge current in actuator coil and the induced current in workpiece. For secondary RL circuit the ordinary differential equation is obtained:

$$\frac{d}{dt}\left(L_1 I_1 + M I_a\right) + R_1 I_1 = 0 \tag{3}$$

where L_1 and R_1 are the self-inductance and electrical resistance of the workpiece respectively.

Magnetic Field

The magnetic vector potential produced by the actuator coil can be computed by applying the Biot-Savart law. The transient discretization in time is needed to evaluate the magnetic field, the density of current in the actuator coil and the workpiece and the electromagnetic forces acting on the workpiece to each variation of the time (Meriched, 2000).

Law of Biot-Savart for Calculation of the Magnetic Field Produced by a Circular Loop at any Point in Space

Figure 2 shows a conductor with circular geometry carrying current "I". Applying the Biot-Savart law the values of magnetic induction at the points p(x,y,z) of the space can be determined mathematically by Eqs. (4), (5) and (6) in Cartesian coordinate system. This calculation is based on the work (Homrich, 2001).

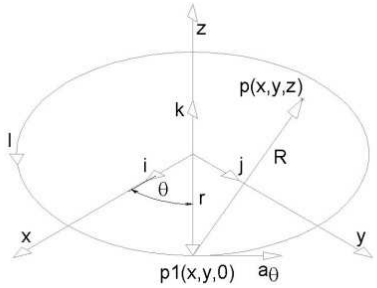

Figure 2. Representation of the circular conductor in cylindrical coordinates.

$$B_x = \frac{\mu_0 I r z}{4\pi} \times$$

$$\times \int_0^{2\pi} \frac{\cos\theta}{\left[x^2 + y^2 + z^2 + r^2 - 2r\left(x\cos\theta + y\sin\theta\right)\right]^{3/2}} d\theta \tag{4}$$

$$B_y = \frac{\mu_0 I r z}{4\pi} \times$$

$$\times \int_0^{2\pi} \frac{\sin\theta}{\left[x^2 + y^2 + z^2 + r^2 - 2r\left(x\cos\theta + y\sin\theta\right)\right]^{3/2}} d\theta \tag{5}$$

$$B_z = \frac{\mu_0 I r}{4\pi} \times$$

$$\times \int_0^{2\pi} \frac{r - y\sin\theta - x\cos\theta}{\left[x^2 + y^2 + z^2 + r^2 - 2r\left(x\cos\theta + y\sin\theta\right)\right]^{3/2}} d\theta \tag{6}$$

Or in cylindrical coordinate system:

$$B_r = \frac{\mu_0 I z r}{4\pi} \times$$

$$\times \int_0^{2\pi} \frac{\cos(\theta - \alpha)}{\left[x^2 + y^2 + z^2 + r^2 - 2r\left(x\cos\theta + y\sin\theta\right)\right]^{3/2}} d\theta \tag{7}$$

$$B_\alpha = \frac{\mu_0 I z r}{4\pi} \times$$

$$\times \int_0^{2\pi} \frac{\sin(\theta - \alpha)}{\left[x^2 + y^2 + z^2 + r^2 - 2r\left(x\cos\theta + y\sin\theta\right)\right]^{3/2}} d\theta \tag{8}$$

$$B_z = \frac{\mu_0 I r}{4\pi} \times$$

$$\times \int_0^{2\pi} \frac{r - y\sin\theta - x\cos\theta}{\left[x^2 + y^2 + z^2 + r^2 - 2r\left(x\cos\theta + y\sin\theta\right)\right]^{3/2}} d\theta \qquad (9)$$

where μ_0 is a magnetic constant equal to $4\pi 10^{-7}$ [H / m].

$$\alpha = arctg\left(\frac{B_y}{B_x}\right) = arctg\left(\frac{y}{x}\right) \qquad (10)$$

Equations (7), (8) and (9) are used to calculate the three components of the vector density of magnetic field B at the point p in cylindrical coordinates. These equations can be solved analytically only for points located in the center of the circular geometry and p(0,0,z). This study uses resident functions in software Matlab for the numerical solution of the integral for the equations above. Figure 3 shows the actual actuator coil and the simplified model with coaxial circular conductors.

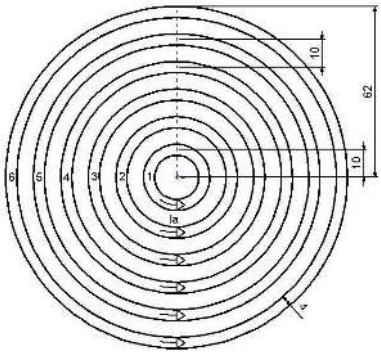

(a)

(b)

Figure 3. Flat spiral coil used in this study: (a) Simplified; (b) Real.

Using differential equations (1), (2), and (3) it can be written the set of ordinary differential equations in matrix form (11). It can be solved by a resident function of the software Matlab after the discretization of the metal sheet in a finite number of conductive windings (Paese, 2010). The calculation of the resistances in (11) is presented (Halliday, 1988).

$$\begin{bmatrix} 0 & 1 & 0 & 0 & 0 \\ 1 & R_a & 0 & 0 & 0 \\ 0 & 0 & R_1 & 0 & 0 \\ 0 & 0 & 0 & R_2 & 0 \\ 0 & 0 & 0 & 0 & R_n \end{bmatrix} \cdot \begin{bmatrix} V_c \\ I_a \\ I_1 \\ I_2 \\ I_n \end{bmatrix} + \begin{bmatrix} -C & 0 & 0 & 0 & 0 \\ 0 & L_a & M_{a1} & M_{a2} & M_{an} \\ 0 & M_{1a} & L_1 & M_{12} & M_{1n} \\ 0 & M_{2a} & M_{21} & L_2 & M_{2n} \\ 0 & M_{na} & M_{n1} & M_{n2} & L_n \end{bmatrix} \cdot \begin{bmatrix} dV_c/dt \\ dI_a/dt \\ dI_1/dt \\ dI_2/dt \\ dI_n/dt \end{bmatrix} = \begin{bmatrix} 0 \\ 0 \\ 0 \\ 0 \\ 0 \end{bmatrix} \qquad (11)$$

Figure 4 shows the magnetic field generated by ampere in the plane of the metal sheet for radial direction. Considering the symmetry of the problem, these values are the same at any radial direction. In Fig. 4 it may be noted that there is a small reduction in the peaks of the radial component of the magnetic field for different workpiece thickness due to difference of the distance between the geometric centers of actuator coil and workpiece.

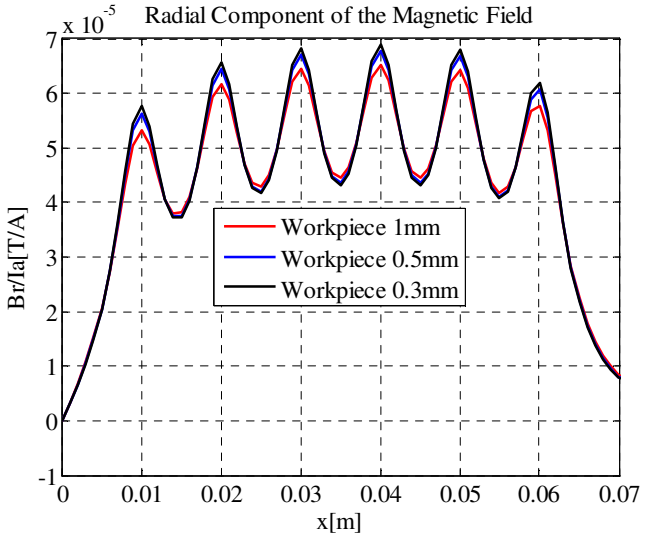

Figure 4. Radial component of the magnetic field from different workpieces thickness.

Calculation of the Self and Mutual Inductances

Considering the flat spiral coil of Fig. 3(a), in which all windings flow the same current I, only the magnetic flux in z direction links the six windings of the coil. The linkage flux and self-inductance can be calculated by (12) and (13) respectively (Paese, 2010).

$$\frac{\lambda}{I_a} = \sum_{i=1}^{n} \Phi_i \qquad (12)$$

$$L_a = \frac{\lambda}{I_a} \qquad (13)$$

The mutual inductance between actuator coil and the nth individual circular conductor of the workpiece and the mutual inductance between its nth individual circular conductors can be calculated by (14) and (15) respectively (Paese, 2010).

$$M_{an} = \frac{N_n \Phi_{an}}{I_a} \tag{14}$$

$$M_{mn} = \frac{N_n \Phi_{mn}}{I_m}; (m \neq n)) \tag{15}$$

Calculation of the Electromagnetic Force

The metal sheet is discretized in coaxial circular elementary conductors (L_1, L_2...L_{12}), where L_1 and L_{12} are the outer diameter and inner diameter respectively. The greater the number of circular elementary conductors the more accurate the model is, but more processing time is needed. The electromagnetic force generated by each circular conductor can be calculated by:

$$Fe_n = B_r I_a I_n C_n \tag{16}$$

where Fe_n, B_r, I_a, I_n, C_n are respectively the force in the n^{th} circular conductor of the workpiece, the magnetic field in radial direction, the discharge current in actuator coil, the induced current in the n^{th} circular conductor of the workpiece, and length of the n^{th} circular conductor of the workpiece.

Parameters of the Electromagnetic Forming System

With the aid of preliminary analysis using mathematical model, a system of electromagnetic forming was developed for deep drawing of thin circular metal sheets by using a flat spiral coil (Geier et al., 2010). More information about the characteristics of the system is shown in Fig. 5 and Table 1, where the resistivities were obtained from (Halliday, 1988).

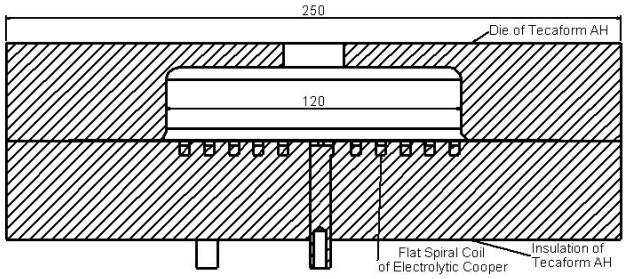

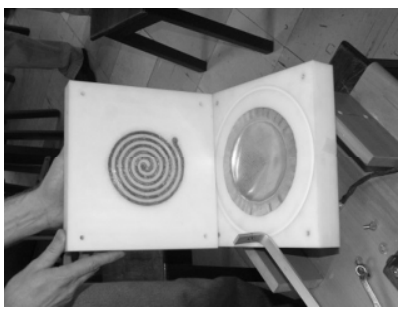

Figure 5. Die of electromagnetic forming device.

In relation to the primary circuit (actuator coil, capacitor banks, main discharge switch and buses) it is noticed that the resistance of the actuator coil is directly related to the Ohm's law, where the greater the number of windings, the greater will be the extension for the electrical current to flow. Regarding to cross section area, it behaves inversely in the calculation of the resistance of the primary circuit. Moreover, the number of windings n and pitch P influences the inductance and magnetic field generated by the actuator coil, since these influence directly in the calculation of the its linkage flux, and consequently the distribution of electromagnetic force (forming force). Also this resistance, inductance and capacitance change the resonant and damping frequencies of the RLC circuit causing a difference of phase between the discharge and induced currents.

Regarding the secondary circuit (workpiece), its parameters as electrical resistances of the discretization of the workpiece (concentric rings) are also influenced by Ohm's law, with electrical resistance being inversely proportional to thickness of workpiece. As well as the primary circuit, the difference of phase between the discharge and induced currents are also dependent on the electrical resistance of workpiece (thickness). This phenomenon is verified in numerical simulation (Matlab) of the set of ordinary differential equations, Eq. (11).

Table 1. System parameters and working conditions.

Equipment	Parameter	Value
Flat Spiral Actuator Coil of Cooper	Number of Windings (n)	6
	Outer diameter (D_0)	120 mm
	Pitch (P)	10 mm
	Cross section (A_a)	16 mm^2
	Self-Inductance (L_a)	1.03 μH (calculated)
	Resistance (R_a)	1.4 mΩ (calculated)
	Resistivity (ρ)	$1.69 \cdot 10^{-5}$ Ω.mm
Bank of Capacitors	Capacitance (C)	8400 μF
	Maximum Voltage (V_c)	900 V
	Maximum Energy (U)	3.4 kJ
Workpiece	Material	Aluminium
	Thickness Analyzed (t)	0.3, 0.5 and 1mm
	Diameter (D_w)	170 mm
	Resistivity (ρ)	$2.75 \cdot 10^{-5}$ Ω.mm
	Gap Between Actuator Coil and Workpiece	1.5 mm

It should have special attention to choice input parameters in order to minimize this phase difference and obtain a magnetic field as uniform as possible. The pitch of the coil actuator has influence in this uniformity of the magnetic field at the same time it is limited by the mechanical rigidity and electrical insulation of the actuator coil (Kamal, 2005).

Results and Discussions

The system of ordinary differential equations and integrates of magnetic field was solved with numerical method in software Matlab, as previously presented. The component in z direction of magnetic field is important to calculate the self and mutual inductances and the component in radial direction is used to calculate the electromagnetic force in z direction (main forming force). The electromagnetic system

shown schematically in Fig. 1 with its parameters given in Table 1 has been simulated and some of the obtained results are shown in the following figures. Figure 6(a) (b) and (c) show the simulated current in the coil (I_a) and the induced current in the workpiece (I_n) which is discretized in twelve circular coaxial conductors, being I_1 the inner one and I_{12} the outer one. Only the induced current in the eighth conductor (I_8), with radius r equal to 40 mm, is displayed as it is the highest induced current.

It may be noted that peak of electric current in the actuator (I_a) remained almost constant for thicknesses of 0.3 mm, 0.5 mm and 1 mm. The biggest change occurs in the induced currents from the elementary circular conductors of the metal sheet, which shows fairly consistent due to the electrical resistance of the elementary conductors being strongly related to its thickness. It is also observed that the difference phase between the discharge and induced currents, which is the highest for the thinnest sheets, and that the discharge occurs more rapidly in the thickest workpiece. Figure 6(d) displayed the measure of voltage in shunt resistor introduced in primary circuit of the system of Fig. 1, although this measure is presented in volts, its profile is directly related to discharge of the coil current (same profile). Using the Ohm's law it is possible to calculate the current that is flowing in the shunt resistor, which can be compared with the simulated one, where an excellent correlation is noted (Fig. 6). This demonstrates that mathematical model and its simplifications are well consistent with experimental results of the discharge current.

Clearly the system behaves as an underdamped RLC circuit and the currents in the actuator coil and workpiece are opposite. The first peaks of the induced currents in 0.3, 0.5 and 1 mm are around –0.38 kA, –0.55 kA and –0.83 kA respectively.

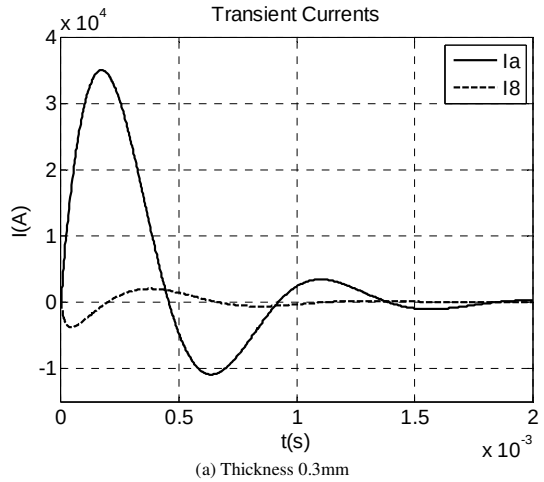

(a) Thickness 0.3mm

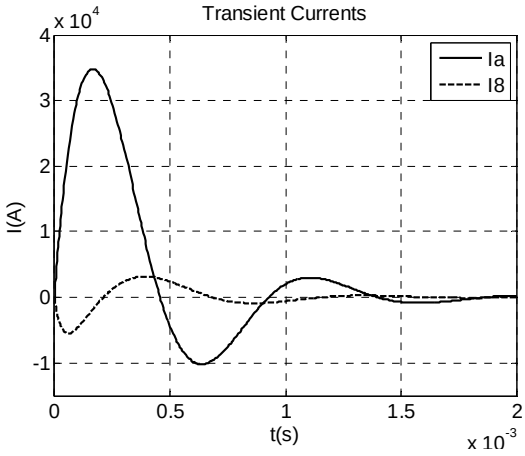

(b) Thickness 0.5mm

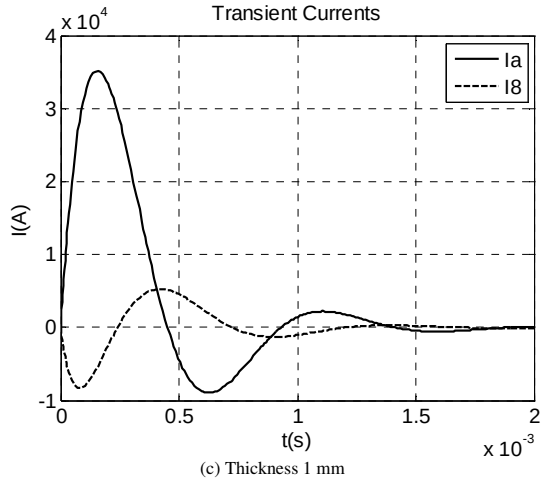

(c) Thickness 1 mm

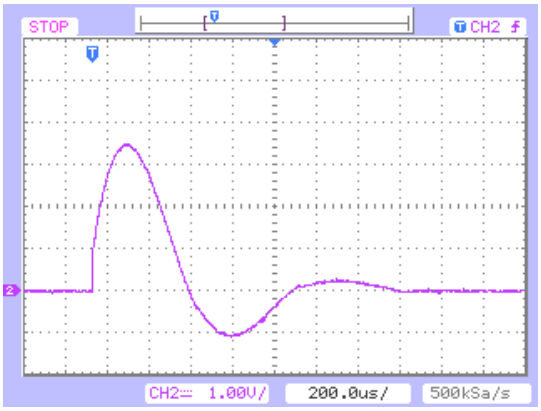

(d) Oscilloscope measurement in shunt resistor (1 volt/div equals to 10 kA/div)

Figure 6. Currents in the actuator coil (solid line) and induced in the workpiece (dashed line): (a) Simulated with workpiece 0.3 mm; (b) Simulated with workpiece 0.5 mm; (c) Simulated with workpiece 1 mm; (d) Voltage in 1 mΩ shunt resistor (1 volt/div equals to 10 kA/div).

Figure 7 shows the axial maximum transient electromagnetic force that occurs in 10^{th} (L_{10}) elementary conductor of the workpiece. It can be seen that considerable forces are developed in this process and the highest difference phase between the discharge and induced currents causes a greater back (attraction) electromagnetic force (negative peak on chart of Fig. 7) when it is compared with electromagnetic force of repulsion (forming force, positive peak on chart of Fig. 7). This shows that back electromagnetic force is the relatively highest for thinnest metal sheets. Again the RLC analogy is satisfied.

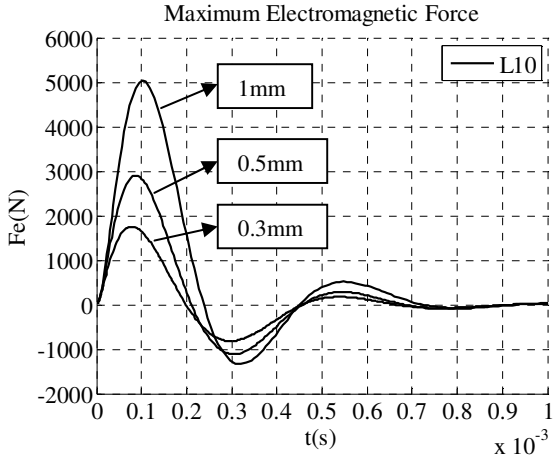

Figure 7. EM force in the 10th circular conductor of the workpiece.

Figure 8 shows the calculated distribution of the repulsive electromagnetic force for axisymmetric problem. The highest values occur where there are windings of the actuator coil and the lowest occur between windings of it. This shows a good correlation with the magnetic field in the radial direction (component used in the calculation of axial force) shown in Fig. 4. It may be noted also that a better distribution would be possible for smaller pitch of the coil actuator, but it weakens the die where the actuator coil is embedded, and the plastic deformation at the plate starts out to the center where the electromagnetic force is equal to zero.

Figure 9 shows the calculated repulsive electromagnetic force (forming force) as a function of the thickness at 10th (radius r equal to 50 mm) elementary conductor of the workpiece for time instants 0.1 ms and 0.32 ms positive and negative peaks on chart of Fig. 7 for a 1 mm workpiece thickness respectively. It may be noted on chart (a) of Fig. 9 that an increase of 233% in thickness (from 0.3 to 1 mm) resulted in an increase of about 177% in the electromagnetic forming force. For the time instant 0.32 ms (negative peak) it may be noted that the back electromagnetic force lowers quickly for workpieces thickness greater than 1 mm. This may explain the occurrence of instability for the experimental workpieces with thickness smaller than 1 mm.

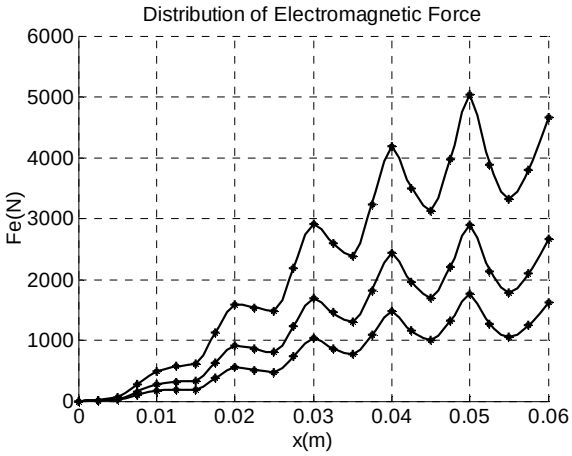

Figure 8. Distribution of the peak repulsive electromagnetic force.

Figure 10 shows experimental results for sheets of different thicknesses. It can be noted certain instability for the thinnest workpiece. One reason for this may be the action of the repulsive electromagnetic force (forming force) that is the lower for the thinner plate and, even though a lower force is required to deform a thinner plate, there is the action of the back electromagnetic force (attraction force) that is relatively high when compared to the repulsive force for the thinner plates, as showed in Fig. 7. This force attracts the plate soon after it is driven (pushed) by the forming force, causing the wrinkling.

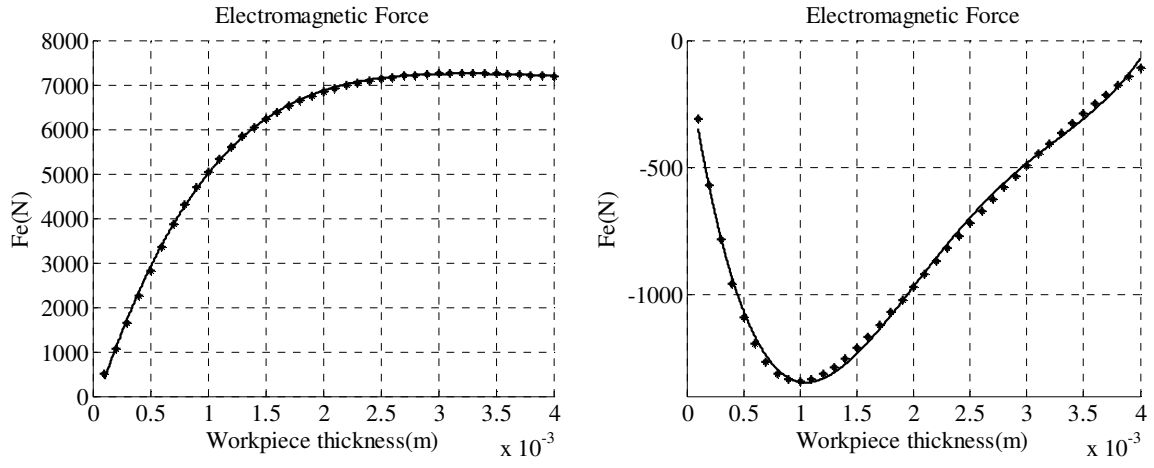

(a) Instant 0.1 ms **(b) Instant 0.32 ms**

Figure 9. EM force in the 10th circular conductor of the workpiece for different thicknesses for time instants 0.1 ms and 0.32 ms.

Thickness 0.3 mm | Thickness 0.5 mm | Thickness 1 mm

Figure 10. Experimental results for different thicknesses.

The presented mathematical model suggests that, since it considers the analysis of the process only for the initial instant before the plastic deformation of the workpiece occurs, this instability is due to the difference of phase between the discharge and induced currents, which are related to input parameters such as thickness workpiece, capacitance and geometry of the actuator coil. This is an issue that currently needs more investigation.

Conclusions

This paper presented a simplified mathematical modeling of an electromagnetic forming system with flat spiral coils as actuator, which allows numerical simulation of the electromagnetic problem before plastic deformation occurs. Experimental results showed that the simplifications made to the model are valid, since there was a satisfactory correlation between experimental and calculated data for discharged current, allowing the identification of parameters and their influence on the process, being the workpiece thickness one of the most critical for the analyzed configuration. Moreover, in this algorithm the theory used is easily identified, facilitating the understanding of the electromagnetic problem and input parameters can be easily modified in order to obtain adjustments or selection of more suitable components for a certain situation. This model also serves as a basis for designing electromagnetic forming systems, which includes an electromagnetic forming machine (capacitors, buses, switches…), a flat coil actuator and its mold retainers since it provides fairly good peak values of discharged and induced currents and the calculation of axial and radial forces of the transient magnetic field. For future work we intend to continue investigations with the construction of a new system in order to experimentally verify the proper parameters to minimize forming instability (wrinkle) in thin plates.

Acknowledgements

This work is based partially on the results of the Master of Science Dissertation by Evandro Paese. The authors would like to thank the following persons: Eng. Michael S. Ertle from TDK-EPCOS for donating the capacitors; Msc. Eng. Luis Fernando Folle for donating aluminium sheets; Eng. Augusto Nienow from Ensinger Engineering Plastics for donation of polyoxymethylene block; Eng. Eliseu Silveira Brito for milling the actuator coil and dies, and Eng. Marcio Migliavacca from Rexfort for milling the spark-gap parts.

References

Boutana, I., Mekideche, M.R., 2008, "Simulation of aluminum sheet electromagnetic forming with several dies", 5th International Multi-Conference on Systems, Signals and Devices (IEEE SSD'08), Amman, Jordan, pp. 1-6.

Geier, M., Paese, E., Pacheco, J.L., Honrich, R.P., Ortiz, J.C.S., 2010, "Proposal for a Test Bench for Electromagnetic Forming of Thin Metal Sheets", in: 4th International Conference on High Speed Forming, Columbus, Ohio/USA. ICHSF2010 – 4th International Conference on High Speed Forming, pp. 264-273.

Halliday, D., Resnick, R., 1988, "Fundamentals of Physics", 3rd edition, Extended Version. Published by John Wiley & Sons, Inc.

Homrich, R.P., Ruppert F.E., Pinatti, D.G., 2001, "Helicoidal single-layer cylindrical coil self-inductance evaluation: a didactic method", Education, IEEE Transactions, Vol. 44, No. 2, pp. 6.

Kamal, M., 2005, "A uniform pressure electromagnetic actuator for forming flat sheets", Dissertation of Graduate Program in Materials Science and Engineering School of the Ohio State University, Columbus, USA, 261 p.

Lange, K., 1985, "Handbook of Metal Forming", Ed. McGraw-Hill, New York, USA, 700 p.

Mamalis, A.G., Manolakos, D.E., Kladas, A.G., Koumoutsos, A.K., Ovchinnikov, S.G., 2006, "Electromagnetic forming of aluminum alloy sheet using a grooved die: numerical modeling", *The Physics of Metals and Metallography*, Vol. 102, Suppl. 1, pp. S90–S93.

Meriched, A., Feliachi, M., Mohellebi, H., 2000, "Electromagnetic forming of thin metal Sheets. Magnetics", IEEE Transactions on, Vol. 36, No. 4, pp. 1808-1811.

Motoasca, T.E., 2003, "Electrodynamics in Deformable Solids for Electromagnetic Forming", Ridderprint Offsetdrukkerij B.V., Netherlands, 236 p.

Paese, E., 2010, "Electromagnetic Forming of Thin Metal Sheets: Technical Feasibility", MSc Thesis (in Portuguese), Universidade Federal do Rio Grande do Sul, Porto Alegre, Brazil, 124 p.

Shang, J., 2006, "Electromagnetically assisted sheet metal stamping", Dissertation of Graduate Program in Materials Science and Engineering School of the Ohio State University, Columbus, USA, 224 p.

Takatsu N., Kato M., Sato K., and Tobe T., 1988, "High speed forming of metal sheets by electromagnetic force", *J.S.M.E. International Journal*, Vol. 31, No. 1, pp. 142-148.

Xu, Wei, Fang, H., Xu, Wenli, 2008, "Analysis of the Variation Regularity of the Parameters of the Discharge Circuit with the Distance Between Workpiece and Inductor for Electromagnetic Forming Processes", *Journal of Materials Processing Technology*, 203, pp. 216–220.